Content

Introduction

Humidity is a highly variable parameter in atmospheric processes and it plays a crucial role in atmospheric motions on a wide range of scales in space and time. Limitations in humidity observation accuracy, as well as temporal and spatial coverage, often lead to problems in numerical weather prediction, in particular prediction of clouds and precipitation. The verification of humidity simulations in operational weather forecasts and climate modeling is also difficult because of the lack of high temporal and spatial resolution data. Ground-based Global Navigation Satellite System (GNSS) receivers have been proposed as a possible data source to improve both model validation and the initial model state used in forecasts. The refractive delay of GNSS radio signals measured by ground based receivers is a function of pressure, temperature, and water vapor pressure. The hydrostatic component of the delay can be determined from surface pressure measurements and removed, leaving the non-hydrostatic component of the refractive delay which is nearly proportional to the content of water vapor, hence called the wet delay.

In my graduation work I considered the basic methods of water vapour estimation in the atmosphere using navigation satellite systems, realized the numerical modeling of radio signal propagation in the atmosphere due to estimation the precision of water vapour content measurements by GNSS.

My work consists of four basic chapters. In the first chapter, which is called «Distribution of water vapor in the atmosphere», i consider the main characteristics of water vapour and its spatial-temporal distribution in globe. Then, in the second chapter – «Global Navigation Satellite Systems», the basic systems of satellite navigation and principles of their working are considered. In the third chapter –«Tropospheric delay modeling» i consider the possibilities of GNSS's application for water vapour content measurements and several typical tropospheric models. And in the last chapter «Precision of water vapour content measurements by

GNSS» the precision of total water vapour content measurements by GNSS is estimated.

1 Distribution of water vapor in the atmosphere

Evaporation from the earth's surface is a practically unique process, providing entering of the water vapour into the atmosphere. Water vapour distribution over the earth's surface is not homogeneous and has diurnal and annual variation. For the quantitative description of water vapour content in the atmosphere the following parameters are used.

1.1 The main parameters of air humidity

In meteorology the following hygrometric characteristics are used:

Water vapor partial pressure e – is the pressure, which is water vapour, being in gas mixture, had if it occupied a volume, which is equal to the volume of the mixture at the same temperature.

Humidity deficit D – is the difference between water vapour saturated partial pressure and water vapour partial pressure:

$$D=E-e \hspace{5cm} (1.1)$$

where D –   is the humidity deficit, hPa;

  E –   is the water vapour saturated partial pressure, hPa;

  e –   is the water vapour partial pressure, hPa.

Absolute humidity a - is the mass of the actual water vapour (g) in 1 m^3 of air:

$$a = 217 \cdot \frac{e}{T} \qquad\qquad (1.2)$$

where a –   is the absolute humidity, g/kg;

         T –   is the temperature of the air, K.

Relative humidity RH – is the ratio of actual water vapour partial pressure to the saturated water vapour partial pressure at a given temperature over the flat surface:

where R_H –   is the relative humidity, %;

$$RH = \frac{e}{E} \cdot 100\% \qquad\qquad (1.3)$$

         E –   is the water vapour saturated partial pressure, hPa;

         e –   is the water vapour partial pressure, hPa.

Specific humidity s – is the water vapour mass (g or kg) in one kilogram of humid air:

$$s = \frac{0.622 \cdot e}{P} \qquad\qquad (1.4)$$

where s –   is the specific humidity, g/kg;

         P –   is the atmospheric pressure, hPa.

Dew point T_d – is the temperature at which the water vapour containing in the air becomes saturated at the constant pressure. It is determine by the amount of water vapour in the air, (K).

Dew point deficit d – is the difference between air temperature and the value of dew point:

$$d = T - T_d \qquad\qquad (1.5)$$

where d –   is the dew point deficit, K;

        T_d –   is the dew point temperature, K.

1.2. Spatial distribution of water vapor in the atmosphere

Distribution of water vapour over the globe depends upon the evaporative rate and water vapour transfer by air currents from one place to another. Characterizing air humidity by its elasticity (water vapor partial pressure), it is possible to notice that distribution of the water vapour partial pressure connects with temperature distribution: the highest values are observed near the equator and they decrease to poleward. Near the equator the mean value of water vapor partial pressure is equal to 25 hPa and it decreases up to 4 - 5 hPa toward 65 - 70N (see table 1.1). [1] It is clear, that in summer decreasing of air humidity toward the high latitudes is larger then in winter time. In winter, near 65 - 70N at low temperature conditions (-20^{0}C and less) water vapor partial pressure is equal to 1 hPa.

Table 1.1 – Mean values of water vapor partial pressure and relative humidity

Parameter	$\varphi^0 N$						
	5	15	25	35	45	55	65
$t, {}^0C$	25.5	25.4	21.9	15.3	8.7	1.2	-7.0
e, hPa	25.3	22.9	18.4	12.9	9.3	6.5	4.1
$f, \%$	79	75	71	70	74	78	82

Variation of air humidity with latitude is more difficult process. Increase in relative humidity near to the high latitude in winter time is typically for moderate area. Near the equator due to high values of water vapour partial pressure the

quantity of relative humidity is high too. In average, during the year, it is equal 85% (see figure. 1.1).

Air humidity is also different along parallels. The highest values of relative and absolute humidity are observed over the oceans and they decrease with moving away from oceans to the continents. Over the continents the distribution of air humidity is not homogeneous and defines by local conditions.
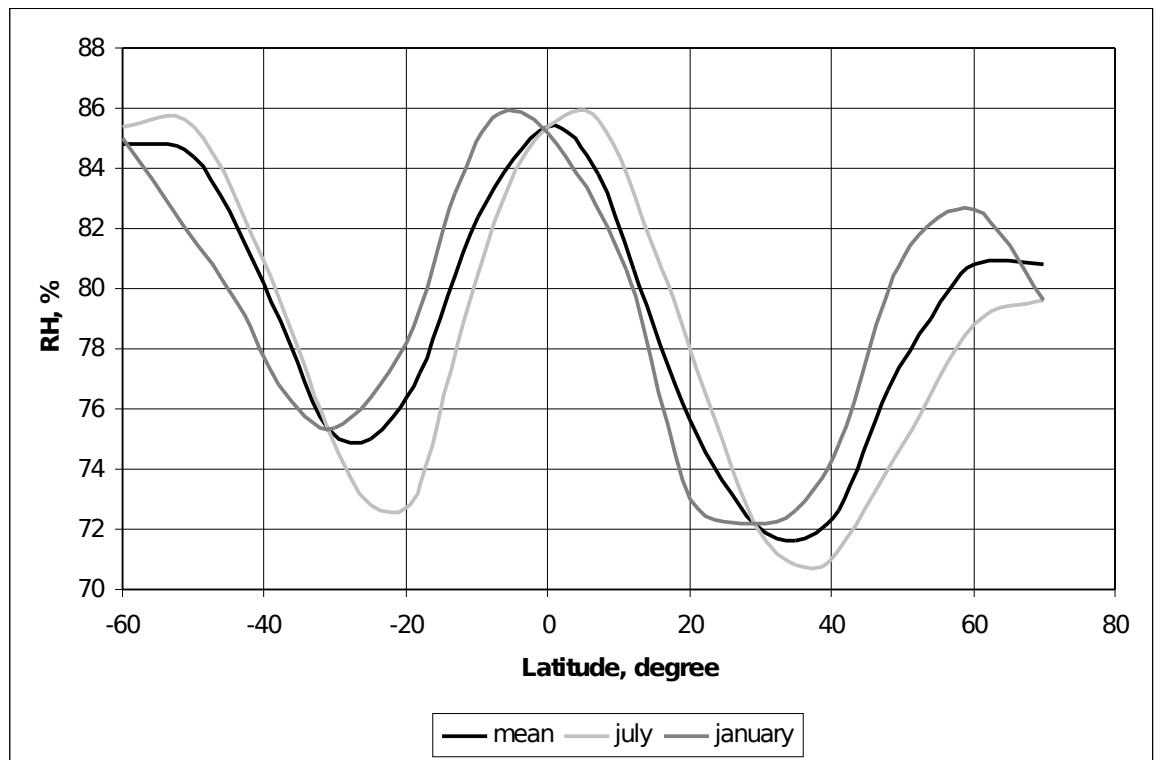

Figure 1.1 – Zonal variation of relative humidity [1]

1.3 Diurnal and annual variation of air humidity

In the surface layer variation of water vapor partial pressure follows out of the temperature one, but variation of relative humidity is reverse to temperature variation. In this layer variation of humidity depends upon water vapor transfer due to vertical exchange. Water vapor content over the surface increase and its temporal variation depends upon only evaporation from the underline surface in case of weak

vertical exchange. Intensive vertical exchange decrease absolute humidity near the surface and therefore the water vapor content at the upper levels increase. All this process determine diurnal variation of air humidity.

Two types of water vapor partial pressure diurnal variation are known. The first type is the similar to temperature variation: diurnal's maximum comes at the same time of temperature maximum, minimum – before a sunrise; amplitude increases together with increase of temperature amplitude (see fig. 1.2). This type will occur at an insignificant vertical exchange and an intensive evaporation. It is observed at those places, where plenty of moisture provides possibility of continuous evaporation. Such diurnal variation usually takes place over the vast water surfaces and above continents in winter time. The second type of diurnal variation is given by double wave and characterized by two maximums: near 9-10a.m and 20-21p.m and two minimums: early in the morning and in the period of the most developed turbulence, at postmeridian o'clock. Such diurnal variation usually takes place over the continents in summer (see fig 1.2).

Diurnal variation of relative humidity depends upon the diurnal variation of water vapour partial pressure and saturated water vapour partial pressure. The increase of temperature influences on the evaporative rate (it increases), therefore the water vapour partial pressure increases too. But saturated water vapour partial pressure goes up much faster, than water vapour partial pressure; therefore with temperature rising, relative humidity decreases and near the surface has diurnal variation, which is reverse to temperature variation. At the continental conditions diurnal lowering of relative humidity is especially sharply expressed in summer. In this case the decrease of water vapour partial pressure due to vertical exchange and increase of saturated water vapor partial pressure due to temperature rising are the reasons of the relative humidity diminishing. Therefore the amplitude of diurnal fluctuation of relative humidity is greater over the land surfaces than over the water surfaces. Maximum in diurnal variation of relative humidity comes before a sunrise, and minimum - near at 15-16 o'clock.

Annual variation of absolute humidity and relative humidity has a simple feature: variation of absolute humidity repeats the variation of temperature; variation of relative humidity is reverse to it. In summer absolute humidity has the largest values and relative humidity has the lowest one; in winter time – vise verse. Thus, in north latitudes – relative humidity is large; it is about 80-90%, in summer it decreases up to 60-70%. Values of water vapor partial pressure is not so high in winter time – 2-3 hPa, in summer it is larger – 12 - 15 hPa, so the annual amplitudes is equal to 10-12 hPa.
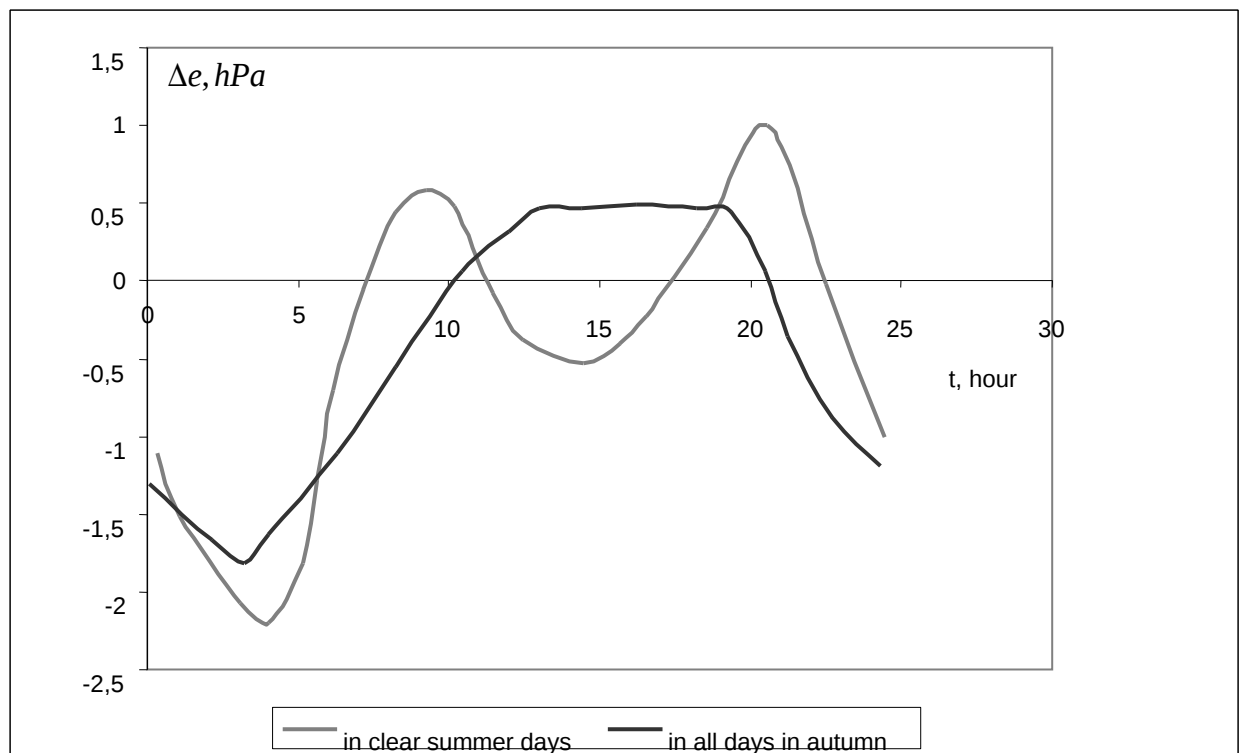

Figure 1.2 – Diurnal variation of water vapour partial pressure [1]

1.4 Distribution of the air humidity characteristics with height

Water vapour enters to the atmosphere from an active surface. As a result of turbulent mixing water vapour spreads into the higher layers of the atmosphere and gets to the stratosphere. Water vapour vertical distribution depends upon the temperature and pressure variation with height, stage of the convection development, turbulent mixing, condensation processes and clouds formation processes. So, vertical distribution of water vapour is not very simple question due to difficult conditions which are defined it.

Observations show that water vapour partial pressure decreases with height according to the formula:

$$e(z) = e_0 \cdot 10^{-\beta/z},\qquad\qquad (1.6)$$

where e_0 –   is the water vapor partial pressure near the surface, hPa;

   β –   is the empirical coefficient (depends upon the geographical region);

   z –   is the height, m.

From the formula (1.6), it is obviously, that water vapor partial pressure decreases with height according to the exponential law.

But the real distribution of the water vapor parameters with height can be significant differ from those which is calculated using empirical formulas. Vertical distribution of water vapor partial pressure is dissimilar: its decrease can be alternate with its increase (for example in the inversion layer).

1.5 Total content of water vapour

In the previous part (1.4) the distribution of the air humidity characteristics with height is considered. From the formula (1.6) as it was noticed, water vapor partial pressure decreases with height according to the exponential low. The coefficient β can be founded from observation's data. For the lowest part of the atmosphere β is approximately equal 5000 m, from this fact it is follows that water vapor partial pressure decreases in 10 times up to 5 km , in 2 times – up to 1.5 - 2 km. Thus the water vapor partial pressure decrease in vertical direction proceeds more quickly than the decrease of total atmospheric pressure. Water vapor concentration decreases with height according to exponential law too.

Consequently, water vapor content decreases with height very rapidly and at the high of 8-10 km its value becomes very small; at the large heights, as a rule, the air is dry enough. However, it does not exclude the possibility of water vapor accumulation at some heights, where at the certain conditions it will be condensed and clouds can be appeared.

It is possible to find the total content of water vapor W enclosing in the column of the atmosphere with a single section (cm^2) up to the any high (or up to the top of the atmosphere) as an integral function, knowing the law of variation a_z with height:

$$W = \int_0^{\infty} a_z d_z = a_0 \int_0^z e^{-\frac{z}{\beta}} dz \qquad (1.7)$$

where
W _ is the total content of water vapour, mm;
a_z _ is the absolute humidity at the height z, g/kg;
a_0 _ is the absolute humidity at the surface, g/kg.

Distribution of total water vapour content (precipitable water vapour) during sixty years (from 1948-2008) represents on the fig. 1.3. The general decrease of precipitable water from equator to poles is a reflection of the global distribution of temperature, because warm air is capable of holding more moisture than cold air.

There are exceptions in the major desert regions, where the air is very dry despite its high temperature. The most humid region is in the western equatorial Pacific, above the so-called oceanic warm pool, where the highest sea surface temperatures are found.

Measuring of atmospheric water vapor can be got in several ways: by the remote sensing of the atmosphere, from aerological, by indirect methods, based on the parameterizations of vertical water vapour profiles or using method of radio occultation. In the last method as a source of radio signal, the signals from Global Navigation Satellite System can be used. In my bachelor work I will consider measuring of water vapor content using Global Navigation Satellite systems.
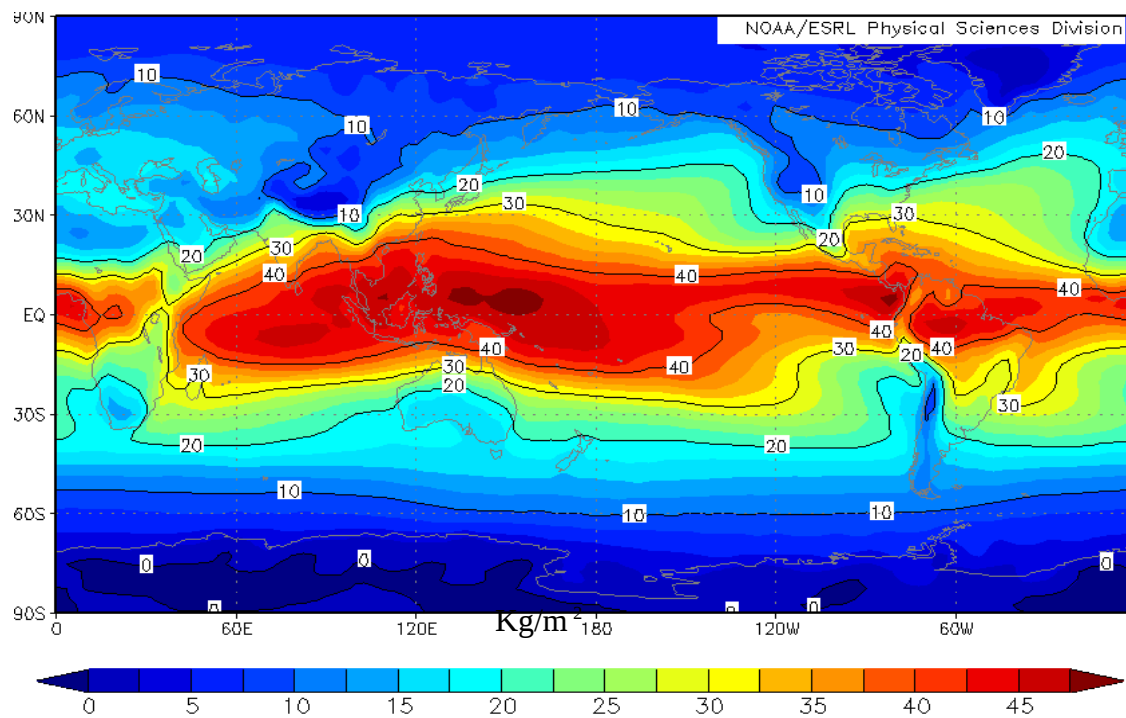

Figure 1.3 – The global distribution of total atmospheric water vapor above the Earth's surface. This depiction includes data from both satellite and weather balloon observations and represents an average for the period 1948–2008 [2]

2 Global navigation satellite system

Satellite navigation systems have become integral part of all applications where mobility plays an important role. Global Navigation Satellite System (GNSS)

involve satellites, ground stations and user equipment, and are now used across many areas of society. There are currently two global systems in operation: the Navigation Satellite Timing and Ranging system (NAVSTAR) commonly referred to as the Global Positioning System (GPS) and owned by the United States of America, and GLONASS (Global Navigation Satellite system) of the Russian Federation. A third system called Galileo is under development by the European Community (EC) countries. Japanese Consortium is also planning to launch a satellite navigation system QZSS.

2.1 Global navigation satellite system components

The GNSS consist of three main satellite technologies: GPS, GLONASS and Galileo. Each of them consists mainly of three segments: space segment, control segment and user segment. These segments are almost similar in the three satellite technologies, which are all together make up the GNSS. In this part GNSS component are considered by the example of GPS.

Space segment:

This consists of the satellite constellation that is orbiting the earth and the Delta rockets used to launch the satellites. In the GPS constellation there are 24 satellites (21 active satellites and 3 reserve satellites) that orbit the earth every 12 hours at an altitude of 20,200 km. The satellites are organized into 6 equally spaced orbital planes (60 degrees apart), with 4 satellites per plane. Each satellite is inclined at 55 degrees to the equatorial plane to ensure coverage of the Polar Regions. [3] A visible explanation of the satellite constellation is provided on the figure 2.1. This combination is designed to provide a user anywhere on the earths surface with $5-8$ visible satellites. The satellites are powered by solar cells, programmed to follow the sun, and have 4 on-board atomic clocks that are accurate to a nanosecond (a billionth of a second). The satellites also have a variety of antennas to generate, send and receive signals. On-board the satellite signals are

generated by a radio transmitter and sent to land-based receivers by L-band antennas.
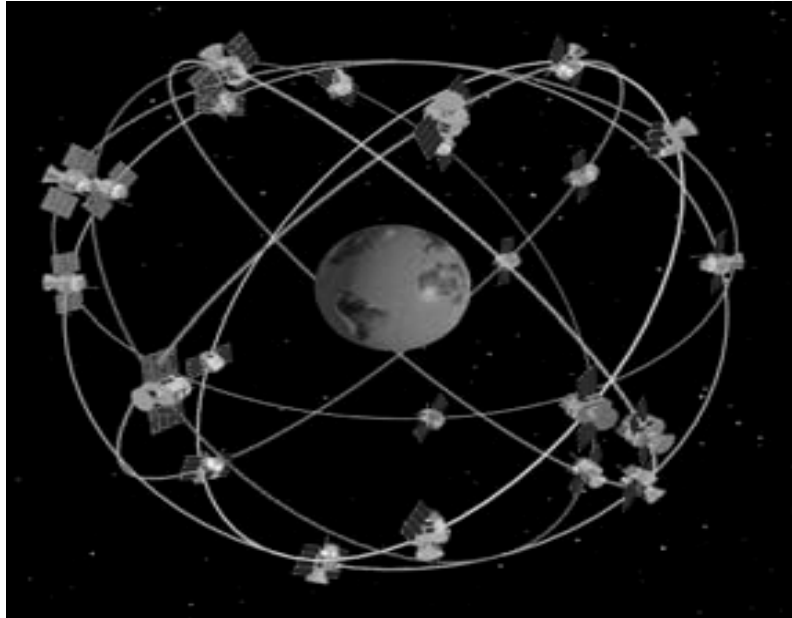

Figure 2.1 – Schematic views of the orbit paths of the GPS satellites

Control segment:

The control segment of the GPS Navigation Systems consists of a Master Control Station which is supported by Monitor Stations and Ground Antennas. The Monitor Stations check the exact altitude, position, speed and overall health of the GPS satellite. A Monitor Station can track up to 11 satellites simultaneously and each satellite is checked twice a day by each Monitor Station. The information collected by the Monitoring Stations is relayed to the Master Control Station to assess the behaviour of each satellites orbit and clock. If any errors are noted then the Master Control Station directs the relevant Ground Antenna to relay the required corrective information to the relevant satellite.

User segment:

The User Segment refers to the civilian and military personnel who use the signals generated by the GNSS satellites. The User Segment consists of the GNSS

receivers and the user community. GNSS receivers convert space vehicle signals into position, velocity, and time estimates.

2.2 Principles of working

2.2.1 Measuring distance

Geo-location using satellite navigation systems is based on the ability to measure the time taken for a signal to travel from a satellite to the receiver. Radio signals travel at the speed of light, which is constant, so if the time of travel is known then the distance between the satellite and the receiver can be determined. Since the position of the satellites is always known, thanks to the work by the Control Segment of the system, an unknown point (the user's receiver) can be calculated if the receiver is obtaining signals from at least four satellites.

GNSS a navigator must know two things, to execute the work. It should know the location of satellites and how far are they from the GNSS navigator (the distance).

We will look at first how a GNSS navigator knows a location place of satellite in space. GNSS navigator gets two types of the encoded information from satellites. One type of information, which is called «almanac", contains information about the satellite position. This information is passing and saving continually in memory of the GNSS navigator, thus the GNSS navigator knows the satellite orbits and where each satellite probably must be. Almanac's data are restored periodically as far as moving of satellite. Any satellite can a bit deviate from its orbit, and the Monitor stations are watching over the orbit, the height, the location and speed of satellite continually. Monitor stations send the data about the satellite orbit to the Master Control station. The Master Control station corrects the data and after the correction sends them backwards to the satellite. This corrected data of exact satellite location is named data of «ephemeris», which are actual during four or six

hours and passed to the GNSS navigator as the encoded information. Thus, getting almanac data and data of «ephemeris», GNSS navigator always knows the location of satellite.

Now GNSS navigator knows the location of satellite, however it must know, the distance between it and satellite, to define its location at the Earth. We can use the simplest formula to calculate the distance: the distance from satellite is equal to the product of the rate of the transmitted signal and the time needed to the signal to pass from satellite to the GNSS receiver. Using this formula, the GNSS receiver knows the rate of the transmitted signal. It is the rate of radiowave, which is equal to 186 000 miles/sec (the speed of light), taking into account the delay of the passing signal through the atmosphere.

Now GNSS navigator must define the temporal constituent of the formula mentioned above. When satellite generates a pseudorandom code, a GNSS navigator generates the same code and tries to co-ordinate its code with the code of satellite. GNSS navigator compares two codes, to determine, as far as it is necessary to delay (or to displace) the code, in order to correspond to satellite's code (see fig. 2.2). In order to get the distance, the time of delay (displacements) is multiplied by velocity of light.

The precision of GNSS navigator's clock is lower than the same on the satellite. Inclusion of the atomic clock in composition of GNSS navigator makes it expensive and increases its prize. Therefore every measurement of the distance requires adjustment on the error size of internal clock of the GNSS navigator. By this reason the measurement of the distance belongs to «pseudo distance». To define the position, using information of «pseudo distance», it is necessary to track and re-count fixed data using four satellites as minimum for removal of error.
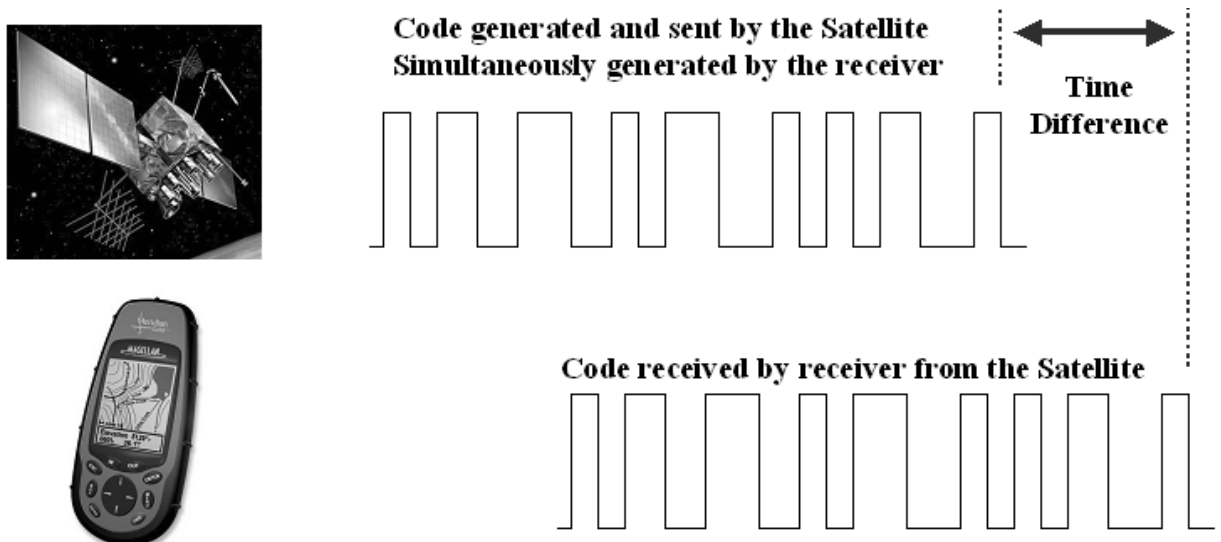
Figure 2.2 – Diagrammatic representation of the C/A code and how it is used to determine time and distance between the satellite and the receiver [5]

2.2.2 Calculating Position

If the distance (r1) from the receiver to a satellite is known then the receiver must be somewhere on a sphere with a radius of d1 that is centered on the satellite. If the distance (r2) to a second satellite is determined then the receiver must also lie somewhere on a sphere of radius r2 centered on the second satellite. Given this knowledge, the receiver must lie on the ellipse that forms the intersection of the spheres. If a third satellite is located then the receiver position is narrowed down to two points where the spheres of the three satellites intersect. Usually one of these positions can be discarded as it is not near the earth's surface. Thus by locating three satellites, the three unknowns in the receiver's location (latitude, longitude and altitude or X, Y, Z) can be determined. However, the determination of the distance between the receiver and satellite relies on very accurate timing. Satellites have very accurate timing due to the use of atomic clocks on-board and constant monitoring by the Control Segment. Unfortunately atomic clocks are too heavy (~20kg) and expensive to mount into GNSS receivers. Therefore GNSS receivers need to use

inferior clocks. This creates a problem as errors in the receiver clock will degrade the estimation of distance by ~300,000 m per millisecond. This problem can be overcome by assuming that the receiver clock error is a fourth unknown in the system. By connecting to a fourth satellite the receiver is able to solve the four simultaneous equations to resolve the four variables (X, Y, Z and clock error) (see fig. 2.3).

a) with a range measurements from one satellite, the receiver is possible somewhere on the sphere defined by the satellite position and the range distance, r

b) with two satellites, the receiver in somewhere on a circle where the two spheres intersect

c) with three satellites the receiver is at one of two points where the three sphere intersect

d) with four satellites, the receiver is at the one point where the four spheres intersect.
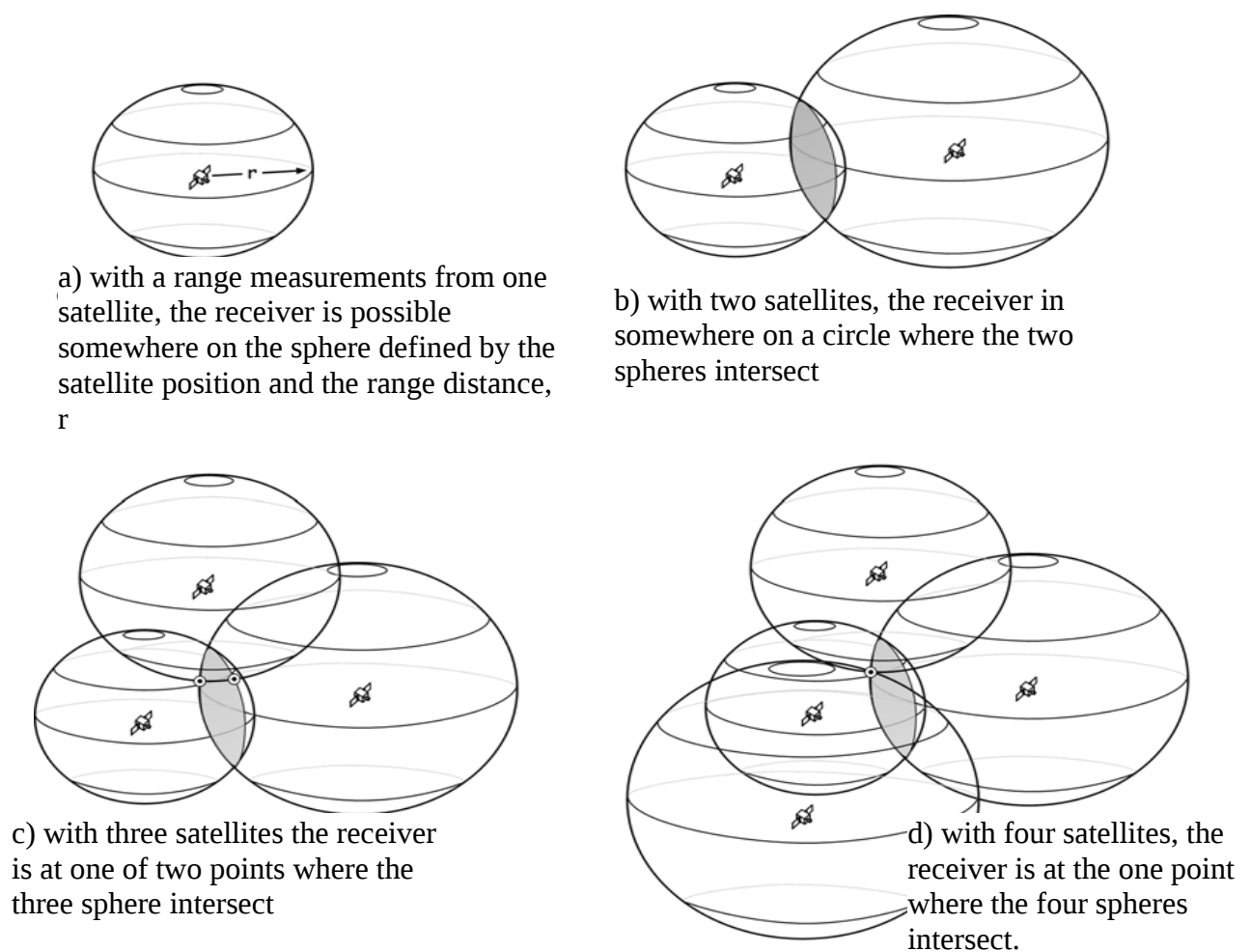
Figure 2.3 – A schematic illustration of how ranging from a receiver to three or more satellites can be used to pinpoint an exact location [5]

2.3 Sources of GNSS signal errors

The GNSS navigator has a potential error in determination of the location as a result of errors from the followings sources:

Signal multi-path — this occurs when the GNSS signal is reflected off objects such as tall buildings or large rock surfaces before it reaches the receiver. This increases the travel time of the signal, thereby causing errors.

Receiver clock errors — a receiver's built-in clock is not as accurate as the atomic clocks onboard the GPS satellites. Therefore, it may have very slight timing errors.

Orbital errors — also known as ephemeris errors, these are inaccuracies of the satellite's reported location.

Number of satellites visible — the more satellites a GNSS receiver can "see", the better the accuracy. Buildings, terrain, electronic interference, or sometimes even dense foliage can block signal reception, causing position errors or possibly no position reading at all. GNSS units typically will not work indoors, underwater or underground.

Satellite geometry/shading — this refers to the relative position of the satellites at any given time. Ideal satellite geometry exists when the satellites are located at wide angles relative to each other. Poor geometry results when the satellites are located in a line or in a tight grouping.

Ionosphere and troposphere delays — the satellite signal slows as it passes through the atmosphere. The GNSS system uses a built-in model that calculates an average amount of delay to partially correct for this type of error.

The troposphere delays can be used to determine the water vapour content in the atmosphere. There are several tropospheric delay models which are considered in the next chapter.

3 Tropospheric delay modeling

GNSS signals have to propagate through the Earth's atmosphere. Two atmospheric regions degrade the quality of GNSS observations: the ionosphere and the neutral atmosphere layer. The ionosphere is a frequency-dispersive medium, that is, the free electrons of the ionosphere cause a frequency dependent phase advance or a group delay to the GNSS signals. However, the neutral atmosphere, which includes the lower part of the stratosphere and the troposphere, is a non dispersive layer. The modeling of this effect on GPS signals requires the information of the atmospheric properties.

3.1 Troposphere composition and structure

The neutral atmosphere layer consists of three temperature-delineated regions: the troposphere, the stratosphere and part of the mesosphere. The neutral atmosphere is often simply referred as the troposphere because in radio wave propagation the troposphere effects dominate with respect to other effects.

The troposphere contains about 80% of the total molecular mass of the atmosphere, and nearly all the water vapor and aerosols. Considering the composition of the troposphere, it can be divided into two parts: dry air and water vapor. Dry air is a mixture of gases, in which nitrogen, oxygen, and argon are the major constituents and account for about 99.95% of the total volume. Dry air is mixed very consistently up to an altitude of approximately 80 km [6]. The main source of water vapor is the evaporation from bodies of water and transpiration by plants. The water vapor content is a function of the local geographic conditions and meteorological phenomenon. Its concentration is less than 1% of the volume of the air in the polar regions and large desert region, but quite significant over tropical rain forests, reaching over 4% of the volume of the air. Therefore, water vapor in the

troposphere is a spatial and temporal variable. Dry air gases, and water vapor in hydrostatic equilibrium, are easily modeled theoretically with the ideal gas law and the hydrostatic equations. Hence, this is the reason to separate the contents of the troposphere into hydrostatic and non-hydrostatic, or wet components. Since the hydrostatic delay is due to the transient or induced dipole moment of all the gaseous constituents of the atmosphere including water vapor, the term

hydrostatic delay is favored over the sometimes used term "dry delay". The hydrostatic delay can be well determined from pressure measurements, and at sea level it typically reaches about 2.3 m in the zenith direction. The zenith wet delay can be less than 10 mm in arid regions and as large as 400 mm in humid regions. Significantly, the daily variation of the wet delay usually exceeds that of the hydrostatic delay by more than an order of magnitude, especially in temperate regions.

3.2 Tropospheric signal delay

When the radio signals traverse the earth's atmosphere, they are affected significantly by variations in the refractive index of the troposphere. The refractive index is greater than unity and it causes an extra path delay. Simultaneously, the changes in the refractive index with varying height cause a bending of the ray. The combination of these two effects is the so-called troposphere refraction of propagation delay. The tropospheric propagation delay is directly related to the refractive index (or refractivity). At each point in the troposphere, the refractive index of a particle of air can be expressed as a function of atmospheric pressure, temperature and humidity. The troposphere propagation delay can be usually divided into hydrostatic and wet components and can be determined from models and approximations of the atmosphere profiles.

The delay experienced by a satellite signal can be determined by integrating the index of the refraction, n, along the signal path, dl :

$$\Delta L_{TR} = \int_0^L (n-1)dl , \qquad (3.1)$$

where ΔL_{TR} – is the tropospheric delay, m;
         L – is the distance passed by the radio signal in the troposphere, m;
         n – is the refraction index of the radio waves;
        dl – is the path of a beam along its trajectory, m.

The refractivity can be determined using the expression presented below:

$$n = 1 + k_1 \cdot R_d \cdot \rho + \left(k_2' \cdot R_v + \frac{k_3 \cdot R_v}{T} \right) \cdot \rho_v , \qquad (3.2)$$

For modeling purposes, the refractivity is often split into a

where k_1 = $7.760 \cdot 10^{-7}$, K/Pa;
       R_d – is the gas constant for dry air;
       ρ – is the density of the air, kg/m^3;
       k_2' =
       R_v – is the gas constant for humid air;
       k_3 =
       T – is the temperature, K;
       ρ_v – is the density of humid air, kg/m^3.

$6.479 \cdot 10^{-3}$, K/Pa ;

hydrostatic and a wet part. In formula (3.2), the first part is the hydrostatic delay, and the expression in the last bracket is the wet delay. The total delay for a satellite signal received at any elevation angle can be

$3.776 \cdot 10^{-3}$, K/Pa;

determined by first estimating the delay for a signal received in the zenith using formula (3.1) and (3.2). The zenith delay is then multiplied by a scaling factor to map the delay down to lower elevation angles.[7] The scaling factor is determined by a mapping

function, and often both a hydrostatic and a wet mapping function are used, so the total delay for a signal received at elevation, can be determined as:

$$ZTD(\beta) = ZHD \cdot m_d(\beta) + ZWD \cdot m_v(\beta) \, , \tag{3.3}$$

where ZTD – is the zenith tropospheric delay, m;
               β – is the elevation angle, degree;
         ZHD – is the zenith hydrostatic delay, m;
            m_d – is the hydrostatic mapping function;
            m_v – is the wet mapping function.

Mapping function – is the ratio of the zenith tropospheric delay under the given angle of elevation to the zenith tropospheric delay under the elevation angle which is equal 90^0. In the simplest case which assumes a flat earth and a constant refractivity, the mapping function follows the "cosecant law" [6]:

$$m(\beta) = \frac{1}{\sin(\beta)} \, . \tag{3.4}$$

But obviously this is not accurate since it depends on assumptions: a flat earth and a constant refractivity.

3.3 The main models of the tropospheric delay

In the past several decades, a number of troposphere propagation models have been reported in the scientific literature. As for the expression in the previous section, the tropospheric propagation delay can be approximated by finding closed-form analytical models for the zenith delay and then by mapping this delay to the arbitrary elevation angles using a mapping function. Much research has gone into the creation and testing of tropospheric refraction models to compute the index of refraction n along the path of signal travel: Saastamonien (1972, 1973), Hopfield (1969). The various tropospheric models differ primarily with respect to the

assumptions made regarding the vertical refractivity profiles and the mapping of the vertical delay with elevation angles.

Saastamonien model

Saastamonien described a standard model for tropospheric delay valid for elevations $\beta \geq 10^0$ and it is given as follows [8]:

For the zenith hydrostatic delay:

$$ZHD = \frac{2.2768 \cdot 10^{-5} \cdot P}{(1 - 2.66 \cdot 10^{-3} \cdot \cos(2\varphi))} - 0.00028 \cdot h, \qquad (3.5)$$

where φ – is the latitude, degree;
       h – is the sea level, m.

For the zenith wet delay:

$$ZWD = \frac{2.2768 \cdot 10^{-4} \cdot \left(\dfrac{1255}{T} + 0.05\right) \cdot e}{(1 - 2.66 \cdot 10^{-3} \cdot \cos(2\varphi) - 2.8 \cdot 10^{-4} \cdot h)}. \qquad (3.6)$$

Hopfield model

For the zenith hydrostatic delay [9]:

$$ZHD = \frac{15.53 \cdot 10^{-8} \cdot P \cdot [40136 + 148.72 \cdot (T - 273.16)]}{T}. \qquad (3.7)$$

For the zenith wet delay:

$$ZWD = (-12.96 \cdot T + 3.718 \cdot 10^5) \cdot 2.2 \cdot 10^{-5} \cdot \frac{e}{T^2}, \qquad (3.8)$$

where e – is the water vapour parsial pressure, Pa;
       T – is the temperature of the air, K.

3.4 Mapping Function models

Over the past 20 years or so, geodesists and radio meteorologists have developed a variety of model profiles and mapping functions for the variation of the delay experienced by signals propagating through the troposphere at arbitrary elevation angles. The simplest mapping function is the cosecant of the elevation angle that assumes that spherical constant-height surfaces can be approximated as plane surface. This is a reasonably accurate approximation only for high elevation angles and with a small degree of bending. The more complex mapping functions are based on the truncation of the continued fractions. This type of mapping function includes Chao, Davis and so on [10]. The mapping functions derived by Davis, Chao and others mapping function are described below.

Projection MappingFunction (PMF)

$$PMF = \frac{1}{\sin(\beta)}. \qquad (3.9)$$

Geometric Mapping Function (GMF)

$$GMF = \frac{-R}{H \cdot \sin\beta} + \frac{\sqrt{(R+H)^2 - R^2 \cdot \cos^2\beta}}{H}, \qquad (3.10)$$

where R – is the average radius of the Earth, 6378000 m;
          H = 50000.

RTCA Mapping Function

$$RTCA = \frac{1.001}{\sqrt{2.001 \cdot 10^{-3} + \sin^2\beta}}. \qquad (3.11)$$

Chao Mapping Function (CMF)

$$CMF = \frac{1}{\sin\beta} + \frac{a}{\tan\beta} + b,$$

(3.12)

where a = 0.00035;

           b = 0.017.

Davis Mapping Function (DMF)

$$DMF = \frac{1}{\sin\beta} + \frac{a}{\tan\beta} + \frac{b}{\tan\beta} + c,$$

(3.13)

where a = $0.001185 + 0.6071 \cdot 10^{-4} \cdot (P - 1000) - 0.147 \cdot 10^{-3} \cdot e -$

                 $- 0.3072 \cdot 10^{-2} \cdot (T - 20) + 0.196 \cdot 10^{-1} \cdot (dT/dz + 6.5) -$

                 $- 0.0564 \cdot 10^{-2} \cdot (h - 11.231);$

       b = $3.333 \cdot 10^{-3} + 1.946 \cdot 10^{-9} \cdot (P - 10^{5}) + 1.747 \cdot 10^{-8} \cdot \sqrt{e} +$

                 $+ 1.040 \cdot 10^{-7} \cdot (T - 288.15);$

       c = -0.009;

   dT/dz – is the temperature grafient, K/m;

      h – Is the sea level, m.

Ifadis Mapping Function (IMF)

$$IMF = \frac{1}{\sin\beta + \dfrac{a}{\sin\beta + \dfrac{b}{\sin\beta + c}}},$$

(3.14)

where
$$a = 1.237 \cdot 10^{-3} + 1.316 \cdot 10^{-9} \cdot (P_0 - 10^5) + 1.378 \cdot 10^{-6} \cdot (T_0 - 288.15)$$
$$+ 8.057 \cdot 10^{-7} \cdot \sqrt{e_0};$$

$$c = 0.078;$$

$$b = 3.333 \cdot 10^{-3} + 1.946 \cdot 10^{-9} \cdot (P_0 - 10^5) + 1.040 \cdot 10^{-7} \cdot (T_0 - 288.15) +$$
$$+ 1.747 \cdot 10^{-8} \cdot \sqrt{e_0};$$

P_0 = is the pressure at the surface;

T_0 = is the temperature at the surface, K;

e_0 = is the water vapour partial pressure at the surface, Pa.

3.5 Total water vapour content estimation

For calculation of the total water vapour content in the atmosphere it is necessary to know the following magnitudes: zenith tropospheric delay, which is measured by GNSS receiver, zenith hydrostatic delay, hydrostatic mapping function and wet mapping function which can be calculated using one of the models mentioned above.

Total water vapour content can be calculated by the following formula:

$$V = \left(k_2' \cdot Rv + \frac{k_3 \cdot Rv}{T_m} \right)^{-1} \cdot \frac{\left[\Delta L_{TR}(\beta) - \Delta L_d(90°) \cdot m_d \right]}{m_v}, \qquad (3.15)$$

where
V – is the total water vapour content, mm;

T_m – is the weighting temperature, K;

m_d – is the hydrostatic maping function;

m_v – is the wet mapping function;

T_m – is the weighting temperature, K.

Weighting temperature can be expressed by the following formula [11]:

$$T_m = \frac{\int\limits_0^\infty \frac{e}{T}\,dz}{\int\limits_0^\infty \frac{e}{T^2\,dz}} \approx 70.2 + 0.72 \cdot T_0 . \tag{3.16}$$

The precision of total water vapour content measurements depends upon the precision of calculation of the magnitudes which are components of the formula (3.15). As it mentioned above, there are different models for calculation. So, it is very important task to choose the more accuracy model and I try to do it in the next chapter.

4 Precision of water vapour content measurements by GNSS

The main goal of the current work is to estimate the precision of the total water vapour content measurements by GNSS.

I have done numerical modeling of the radio signal propagation in the atmosphere using the program. Listing of program is presented in the Appendix A.

I consider free simulation models with different temperature distribution with height (see fig. 4.1).
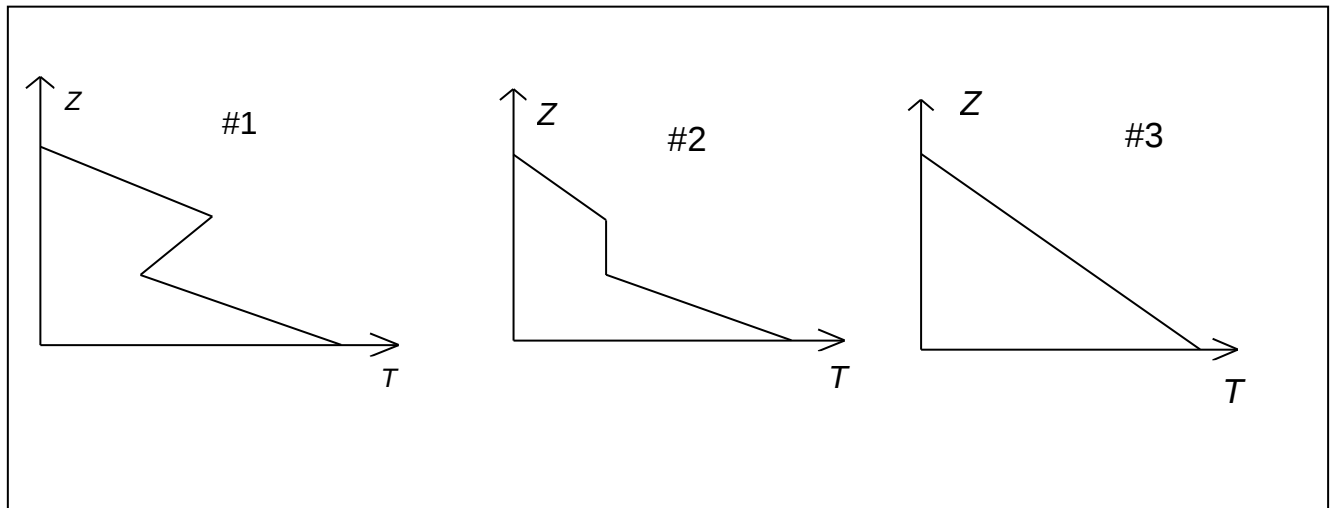
Figure 4.1 – Simulation models

In each simulation model I consider three cases with different initial data (see table 4.1).

Table 4.1 – Initial data

Case	T_0, K	P_0, hPa	e_0, hPa	α, m^{-1}
A	288.15	1013.3	17.0	-1/1500
B	288.15	1013.3	17.0	-1/500
C	253.15	1013.3	1.3	-1/500

Thus, nine different simulation models are received: 1A, 1B, 1C; 2A, 2B, 2C; 3A, 3B, 3C. For each simulation model the zenith hydrostatic delay, hydrostatic mapping functions and wet mapping function were calculated. Using the receiving data the diagrams were made (see Appendix B).

First of all I estimated which of zenith hydrostatic delay models is the more accuracy. Figures B.1, B.2 and B.3 show the absolute error of the zenith hydrostatic delay estimation from the two models. The elevation angle changes from 0^0 to 90^0. The figures show that the values given by the Saastomoinen and Hopfield model are the same. Thus the precision of measurements is the same too. So we can use any one of these models.

Secondary I choose the more accuracy model for hydrostatic mapping function and wet mapping function. Figure B.4, B.5and B.6 show the absolute error of the hydrostatic mapping function estimation from the six models. It is clear from the figures that the lowest absolute error has the RTCA model. Figure B.7, B.8, B.9 show the absolute error of wet mapping function calculated from the six models and in this case the lowest absolute errors has the Projection model.

Now, the total water vapour content can be calculated, using the formula (3.15) and using the models which are chosen above: Saastamoinen model for zenith hydrostatic delay calculation, RTCA model for hydrostatic mapping function calculation and Projection model for wet mapping function estimation.

Figures B.10 and B.11, B.12 show the absolute and relative errors of the tropospheric delay estimation for nine simulation models. The elevation angle changes from 0^0 to 90^0. It is clear from these figures that the precision of measurements depends upon the elevation angle, the more the angle the less the errors of water vapour content measurements. Thus it is possible to make a conclusion that the most convenient elevation angle for measurements is more than 30^0.

If we compare figure B.11 with figure B.12, we could say that the precision of measurements depends upon the amount of water vapour in the atmosphere. So,

the errors are high under the conditions of dry air and lower air temperature. (see fig. B.12).

If we compare the results of modeling for the model #1, model #2 and model#3, we can make conclusion that the lowest errors of total water vapour content calculations are observed for the model #3 (temperature decreases according to the linear law). If we compare Case A and Case B we can say that the errors of measurements depends upon the vertical profile of water vapour distribution.

Thus the most favorable conditions for the total water vapour content estimation are:

- elevation angle is more than 30^0;
- high values of water vapour content in the atmosphere;
- rapid decreasing of water vapour with height;
- temperature decreasing according to the linear law.

Conclusion

As a result of the current graduation work the following conclusions are made:

- The distribution of water vapour in the atmosphere is highly variable function both of time and space and its measurements are very important for numerical weather prediction.

- For water vapour content measurements GNSS can be used. It based on that fact that when a radio signal passes the earth's atmosphere it affects the wave in three ways: it causes a propagation delay; it causes a bending of the ray path; and it absorbed the signal. Propagation delay in the neutral atmosphere is called troposphere delay and can be represented as a sum of two components: hydrostatic and wet. The last component connects with water vapour concentration in the atmosphere. Thus, signal's delay in the troposphere can be used for water vapour content measurements.

- Global navigation satellite system receiver allows to measure total water vapour content over the point of its location, so it can be used as a humidity sensor.

- The precision of total water vapour content measurements depends upon the elevation angle, the amount of water vapour in the atmosphere, the temperature profiles and humidity profiles.

- Ground-based GNSS receivers are an attractive source of humidity data for weather prediction in that they are portable and economic, and provide measurements which are not affected by rain and clouds and they have the advantage of providing automated continuous data.

Listing of program

```java
import java.util.*;
import java.io.*;
import java.net.*;
import java.sql.*;
import static java.lang.Math.*;
import java.util.Locale;

class Path2 {

static String dataBaseUser = "root";
 static String dataBasePassword = "";

 public static void main(String[] args) {

  int i
  int j
  double c = 299792458.0;
  double H = 100000.0;
  double dz = 1.0;
  int N = (int)floor(H/dz)+1;
  int M = 90;
  double k = 1.380662E-23;
  double m = 4.811E-26;
  double g = 9.780318;
  double Rd = 287.054;
  double Rv = 461.526;
  double k1 = 7.760E-7;
  double k2 = 7.040E-7;
  double k3 = 3.739E-3;
  double k21 = k2 - k1*Rd/Rv;
  double[] z;
  double[] T;
  double[] P;
  double[] e;
  double[] n;
  double dT_dz;
  double de_dz;
```

```
double R = 6370000.0;
double beta;
double al;
double d;
double Tm;
double v;

double dLd;
double dLw;
double dL;

double ZHD, ZHD1, ZHD2;
double ZWD;
double Mh,mh1,mh2,mh3,mh4,mh5,mh6,mh;
double Mw,mw1,mw2,mw3,mw4,mw5,mw6,mw;
double V;
String query = null;

Arrays
    z = new double[N];
    T = new double[N];
    P = new double[N];
    e = new double[N];
    n = new double[N];

T[0] = 288.15;
P[0] = 101325.0;
e[0] = 1704.2;

 Troposphere tr = new Troposphere(T[0], P[0], e[0]);

 n[0] = tr.calcRefractiveIndex(T[0], P[0], e[0]);

 for(i=1;i<N;i++) {

    z[i] = i*dz;
 dT_dz = 0;

 if(z[i]< 10000) {
  dT_dz=-0.0065;
  if(z[i]< 500) dT_dz=-0.0065;
  else if (z[i]>=500 && z[i]<700) dT_dz=0.0065;
  else dT_dz=-0.0065;
```

```
   }
   else
    dT_dz=0;

    T[i] = T[i-1] + dT_dz*dz;

   P[i] = P[i-1]*exp(-m*g*dz/(k*(T[i-1]+T[i])/2));
    if(P[i]<0) P[i] = 0;

   de_dz = -1.0/1500.0*e[i-1];
   e[i] = e[i-1] + de_dz*dz;

   n[i] = tr.calcRefractiveIndex(T[i], P[i], e[i]);
    }

  v = e[0]/Rv/T[0] * (z[1]-z[0])/2.0;
 for(i=1;i<N-2;i++)
  { v = v + e[i]/Rv/T[i] * (z[i+1]-z[i-1])/2.0; }
 v = v + e[N-1]/Rv/T[N-1] * (z[N-1]-z[N-2])/2.0;
 Tm = 70.2 + 0.72*T[0];


  System.out.printf(Locale.US,
"******************************************************************
******\n");
  System.out.printf(Locale.US,
  System.out.printf(Locale.US,
  System.out.printf(Locale.US,
"******************************************************************
******\n");
 System.out.printf(Locale.US, "\n");

 for(j=0;j<M;j++) {

 beta = 90.0 - (double)j;

   al = tr.calcRefractionAngle(z, n, beta);
   d = tr.calcRefractionDelta(beta, al, 19100000.0, n[0]);


   dLd = tr.calcHydrostaticDelay(z, T, P, e, beta);
   dLw = tr.calcWetDelay(z, T, P, e, beta);
   dL = dLd+dLw;
```

```
    Mw = dLw / tr.calcWetDelay(z, T, P, e, 90);

  ZHD1 = tr.getSaastamoinenZHD();
  ZHD2 = tr.getHopfieldZHD();
  ZHD = ZHD1;

  ZWD = (k21*Rv+k3*Rv/Tm)*v;

  Mh = dLd / tr.calcHydrostaticDelay(z, T, P, e, 90);
  mh1 = tr.getIfadisHydrostaticMappingFunction(beta);
  mh2 = tr.getRTCAMappingFunction(beta);
  mh3 = tr.getChaoMappingFunction(beta);
  mh4 = tr.getDavisMappingFunction(beta);
  mh5 = tr.getGeometricMappingFunction(beta);
  mh6 = tr.getProjectionMappingFunction(beta);
  mh = mh2;
  Mw = dLw / tr.calcWetDelay(z, T, P, e, 90);
  mw1 = tr.getIfadisWetMappingFunction(beta);
  mw2 = tr.getRTCAMappingFunction(beta);
  mw3 = tr.getChaoMappingFunction(beta);
  mw4 = tr.getDavisMappingFunction(beta);
  mw5 = tr.getGeometricMappingFunction(beta);
  mw6 = tr.getProjectionMappingFunction(beta);
  mw = mw5;
  V = 1.0/(k21*Rv+k3*Rv/Tm) * (dL - ZHD*mh)/mw;

 //**  System.out.printf(Locale.US, "%.0f\t%.3f\t%.3f\n", beta, ZHD1-dLd, ZHD2-
dLd, Mh, mh);
// System.out.printf(Locale.US, "%.0f\t%.3f\t%.3f\t%.3f\t%.3f\t%.3f\t%.3f\t%.3f\t
%.3f\t%.3f\t%.3f\t%.3f\t%.3f\t%.3f\t%.3f\n", beta, ZHD1-dLd, ZHD2-dLd, mh1-
Mh, mh2-Mh, mh3-Mh, mh4-Mh, mh5-Mh,mh6-Mh, mw1-Mw, mw2-Mw, mw3-
Mw, mw4-Mw, mw5-Mw,mw6-Mw);
//    System.out.printf(Locale.US, "%.0f\t%.3f\t%.3f\t%.3f\t%.3f\t%.3f\t%.3f\n",
beta, dLd, ZHD*mh, dLw, ZWD*mw, dL, ZHD*mh+ZWD*mw);
//    System.out.printf(Locale.US, "%.0f\t%.3f\t%.3f\n", beta, abs(V-v), abs(V-
v)/v*100.0);
    System.out.printf(Locale.US, "%.0f\t%.2f\t%.2f\t%.4f\n", beta, abs(V-v), abs(V-
v)/v*100.0, mh/mw);
//   System.out.printf(Locale.US, "%.0f\t%.3f\t%.3f\n", beta, al, d);
  }
```

Appendix B

Diagrams
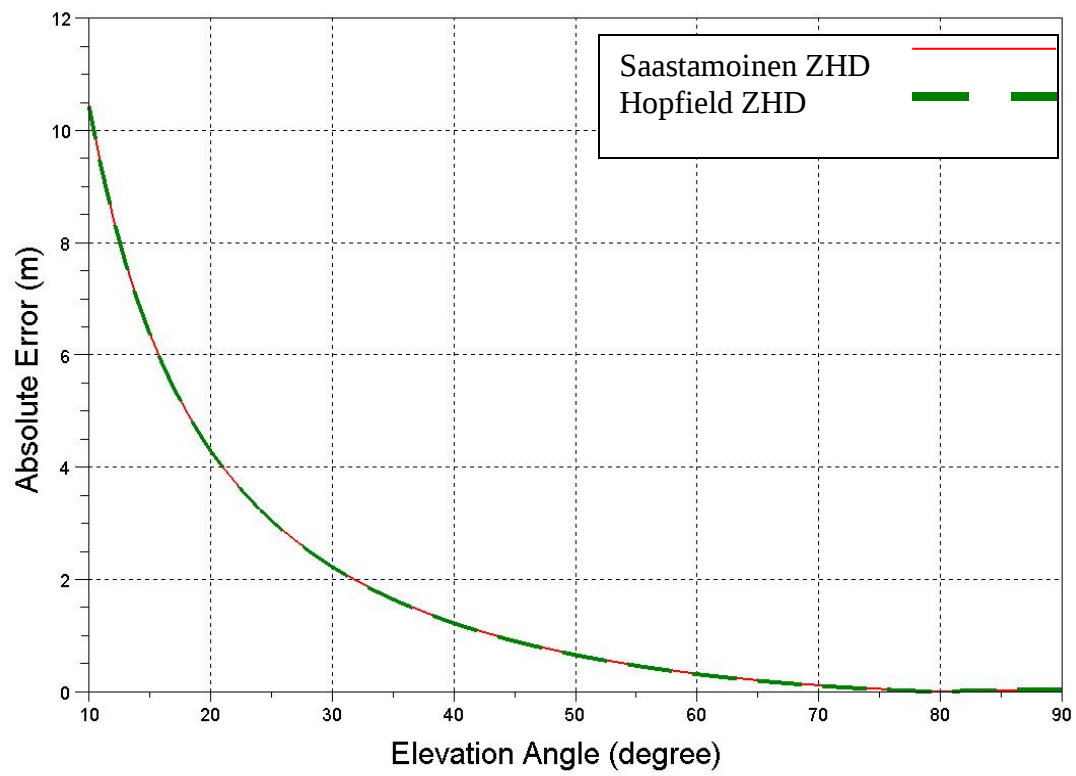
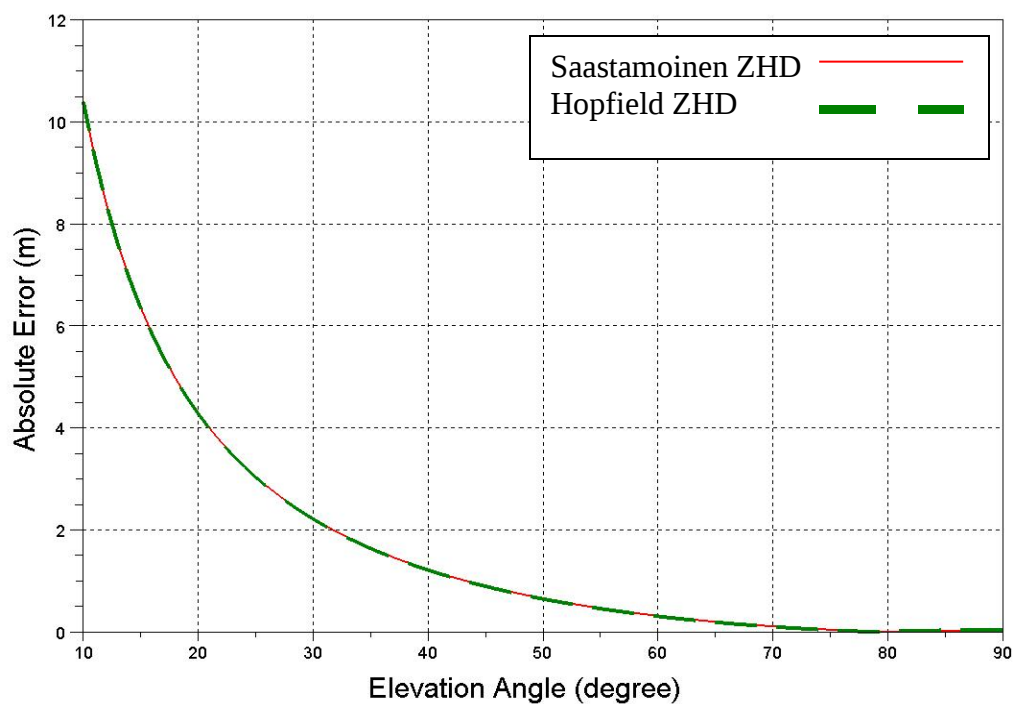Figure B.1 – Absolute Error of the zenith tropospheric delay
for the models 1A, 2A, 3A

Figure B.2 – Absolute error of the zenith tripospheric delay for the models 1B, 2B, 3B
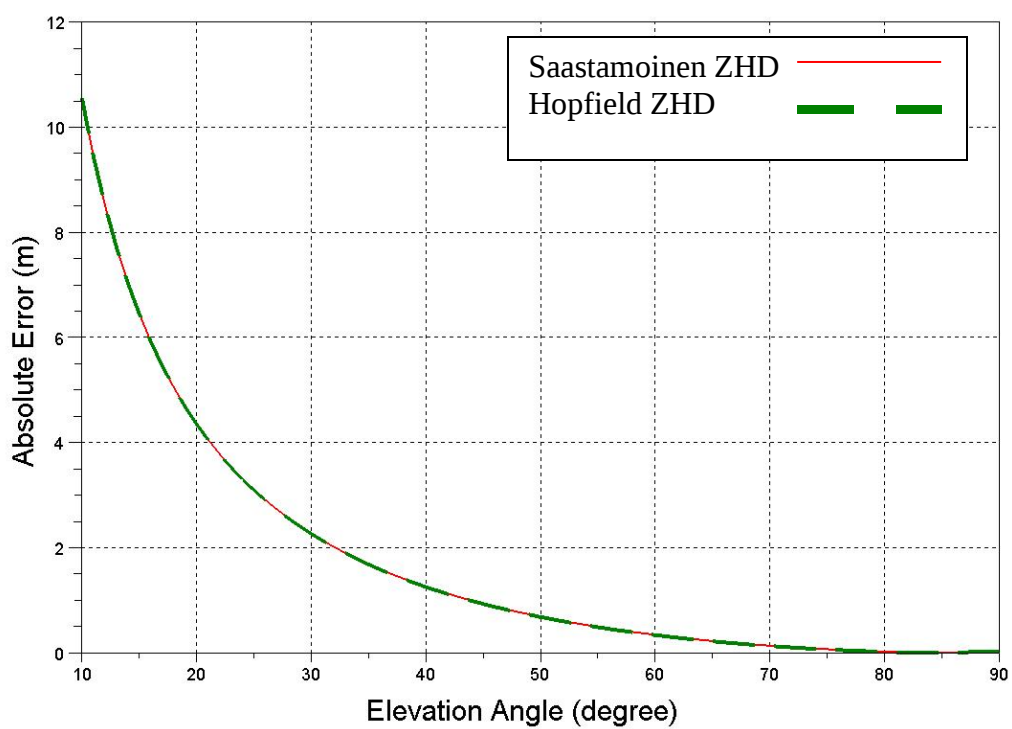

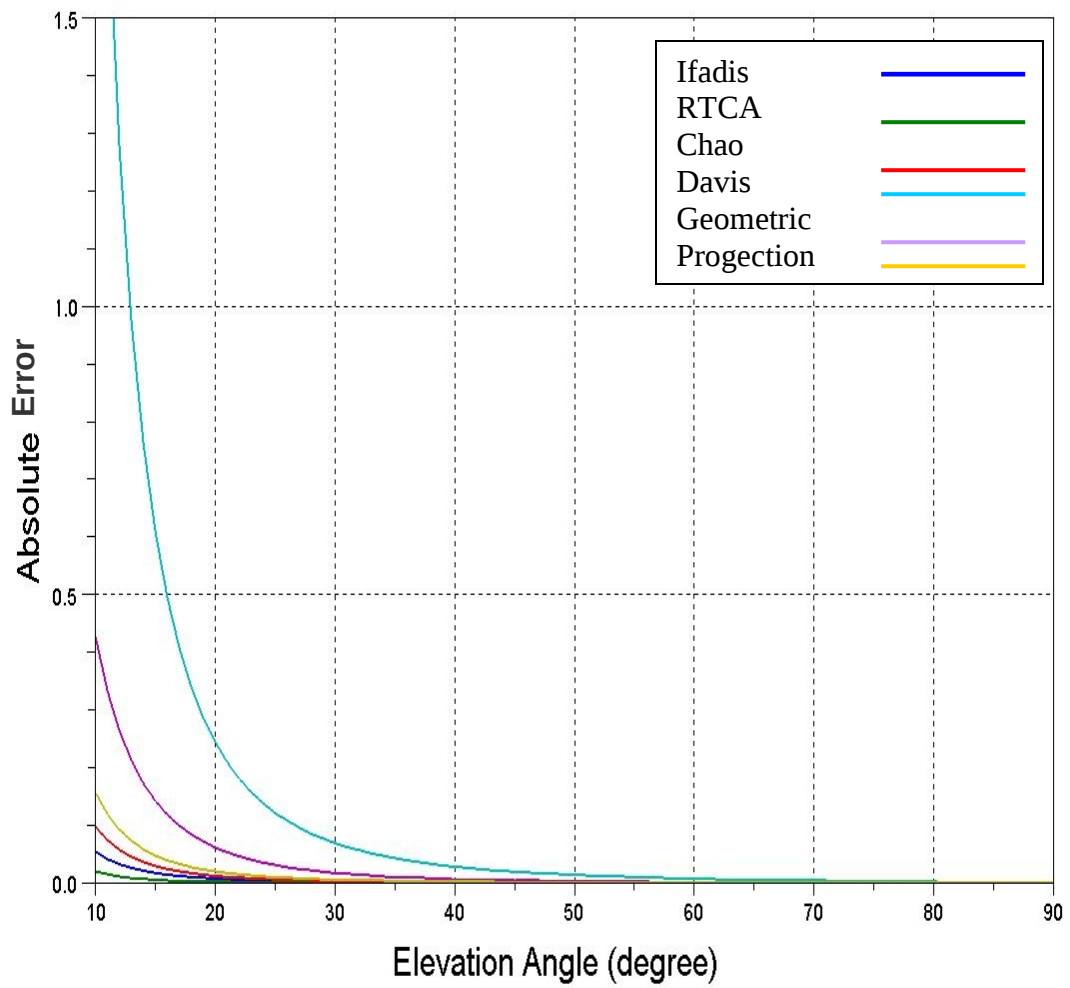Figure B.3 – Absolute error of the zenith tripospheric delay for the models 1C, 2C, 3C

Figure B.4 – Absolute Error of the hydrostatic mapping function
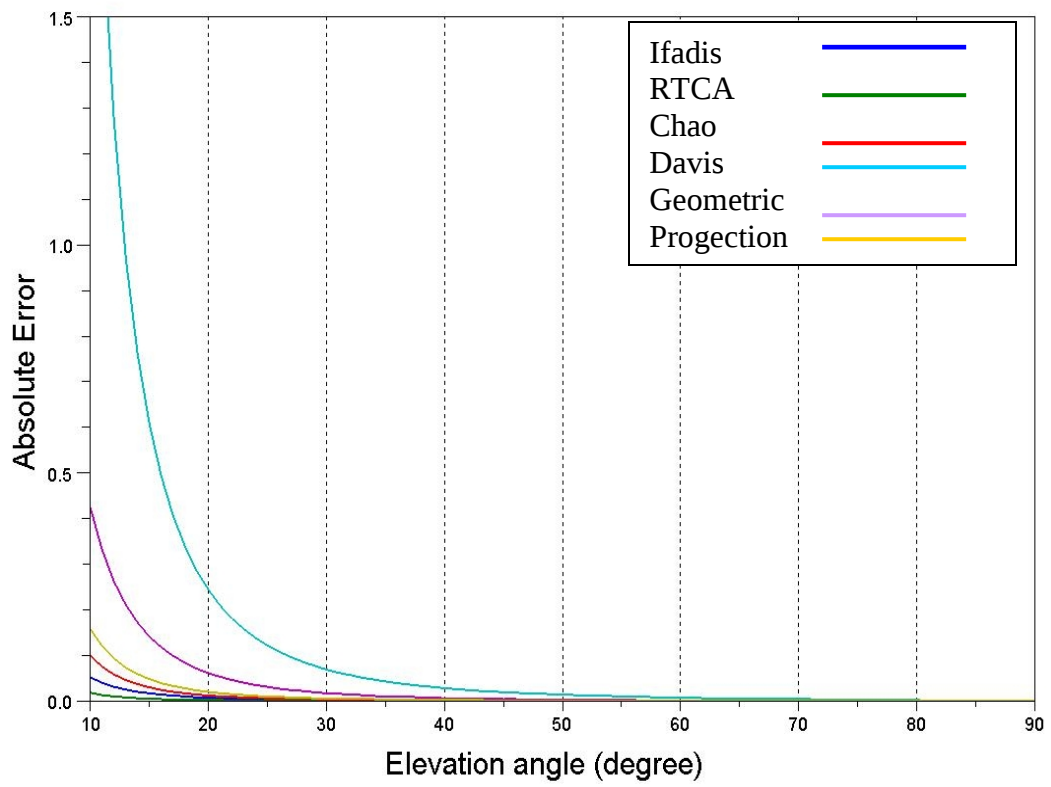for the models 1A, 2A, 3A

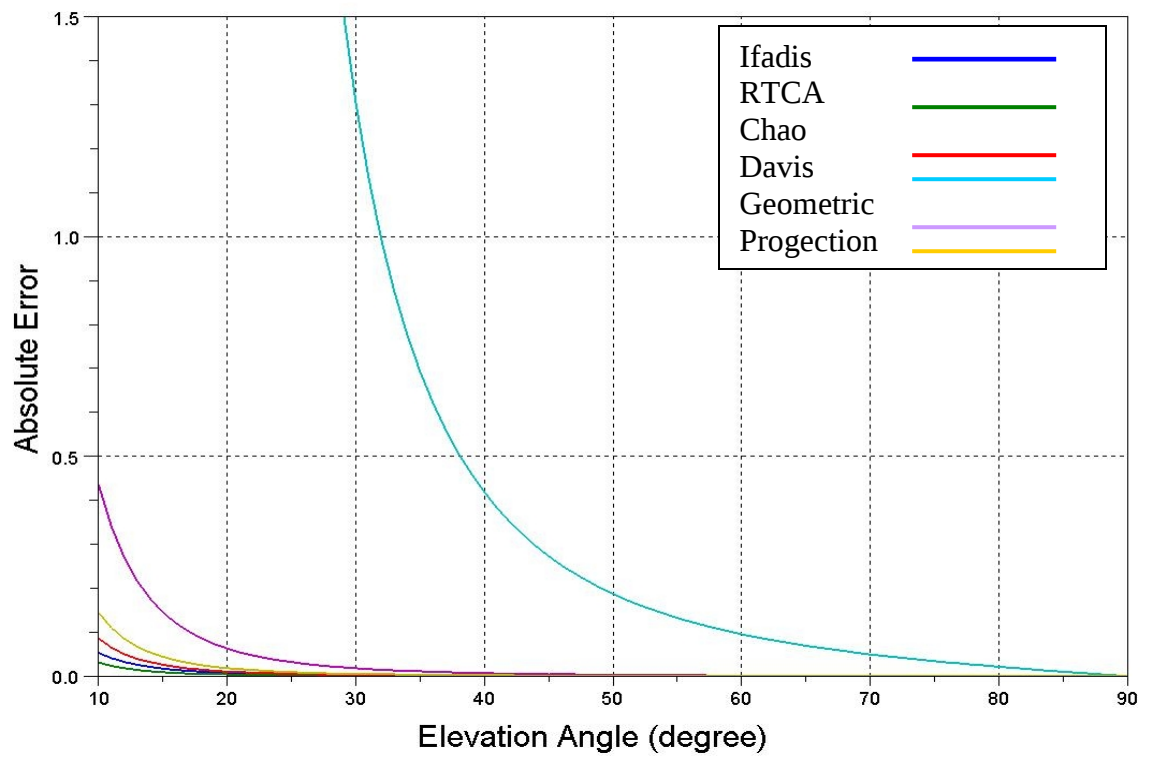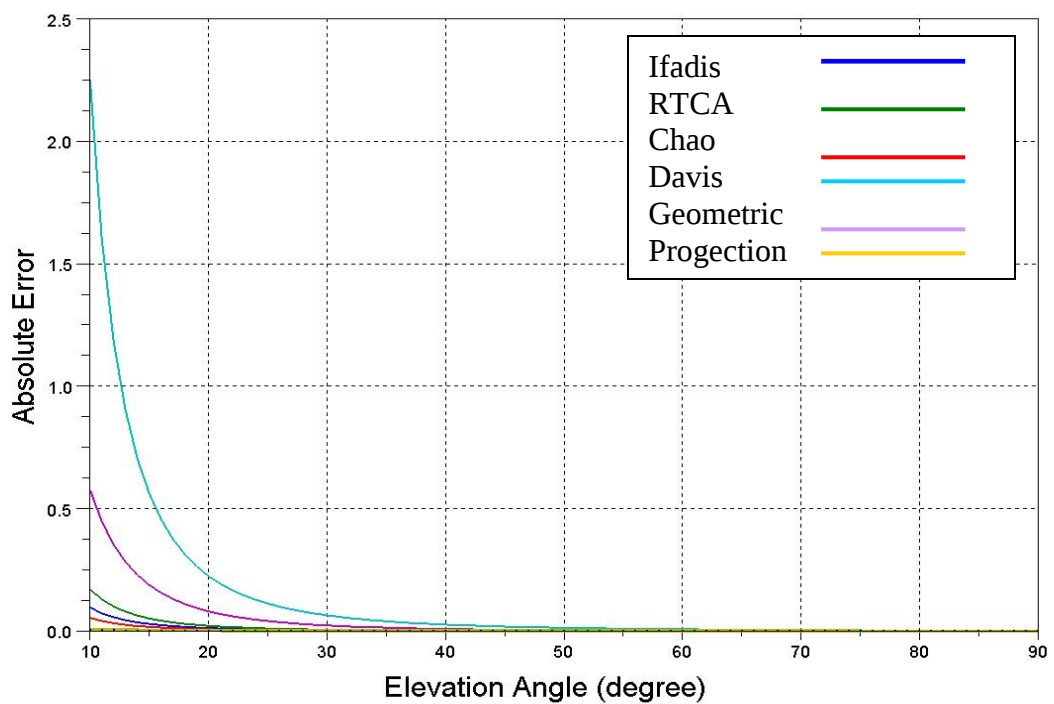Figure B.5 – Absolute error of the hydrostatic mapping function
for the models 1B, 2B, 3B

Figure B.6 – Absolute error of the hydrostatic mapping function
for the models 1C, 2C, 3C

Figure B.7 – Absolute Error of the wet mapping function for the models 1A, 2A, 3A
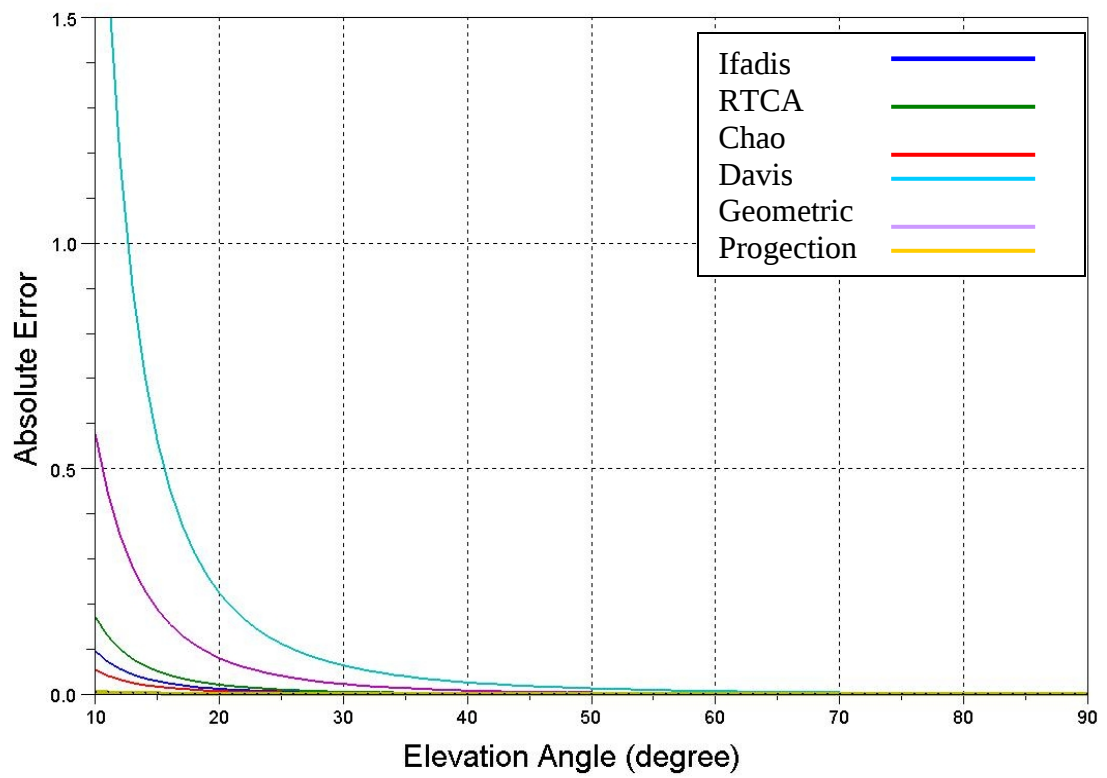
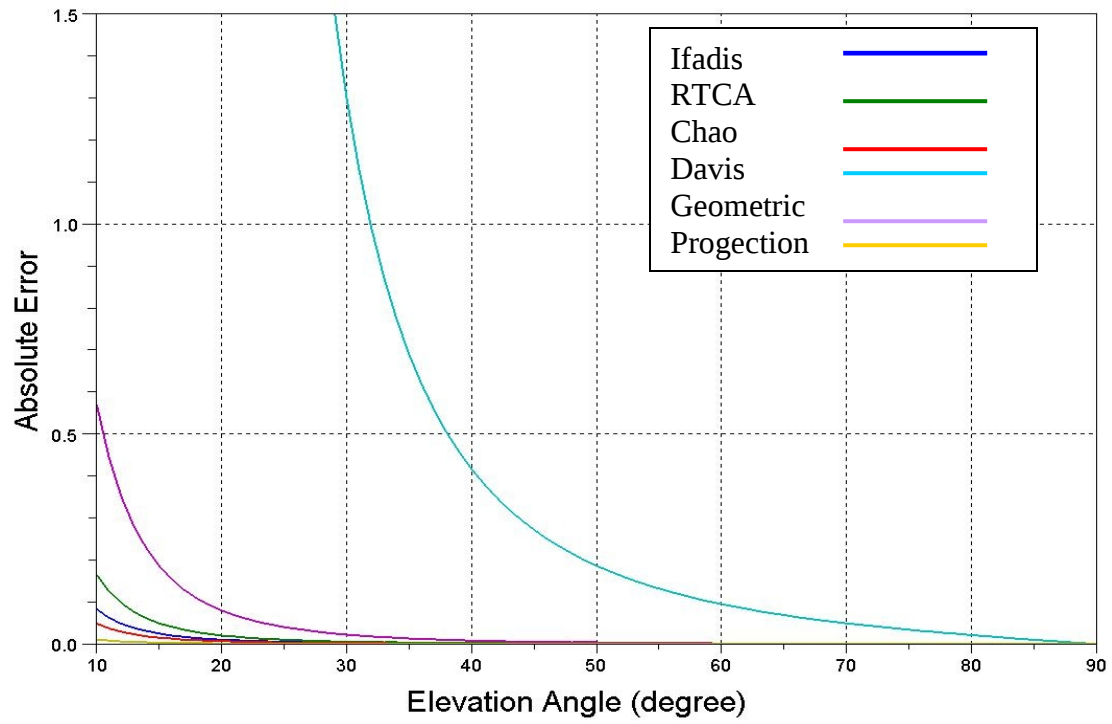Figure B.8 – Absolute Error of the wet mapping function for the models 1B, 2B, 3B

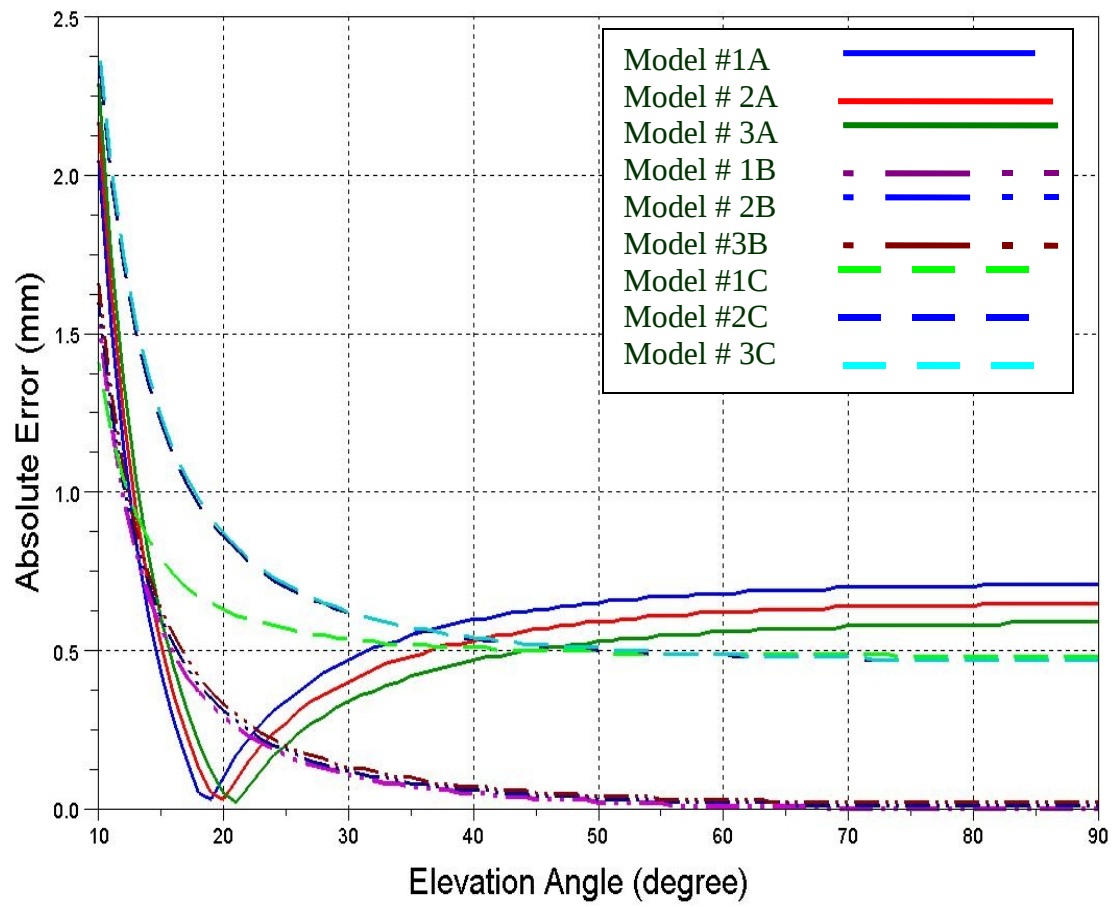Figure B.9 – Absolute error of the wet mapping function for the models 1C, 2C, 3C

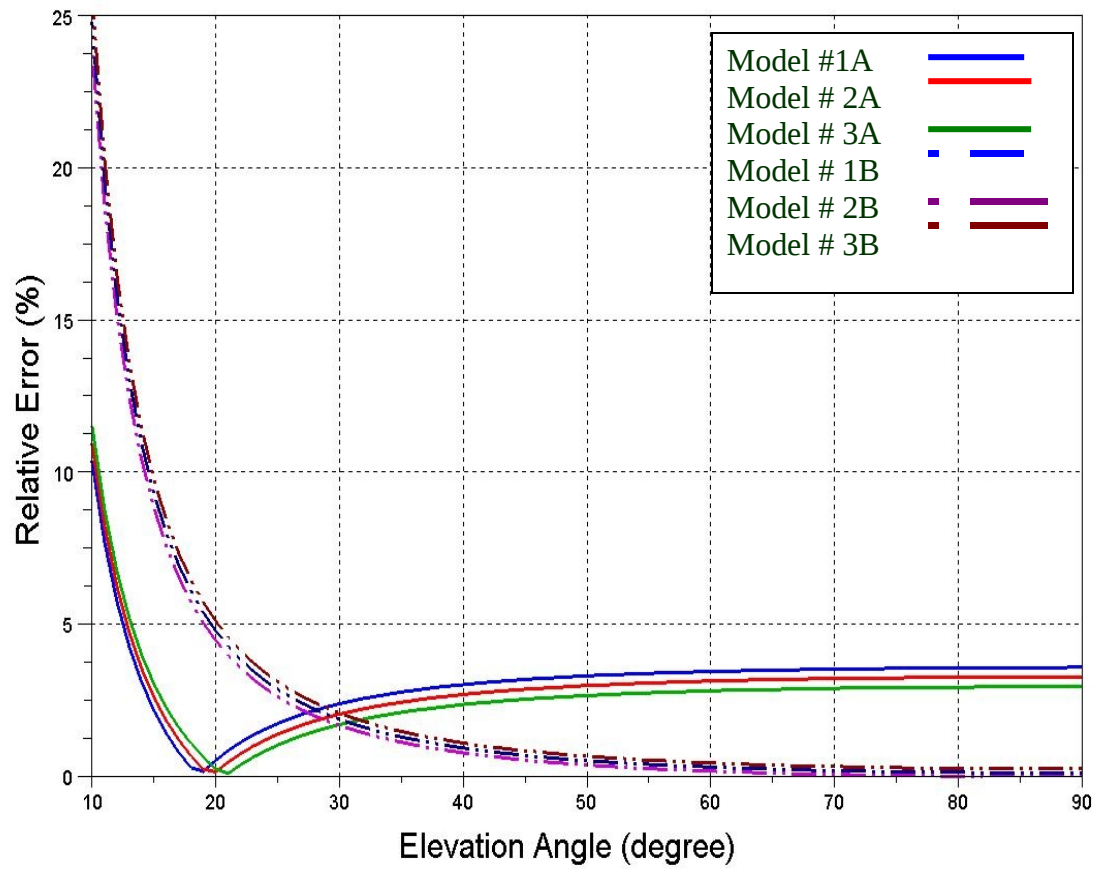Figure B.10 – Absolute error of the total water vapour content

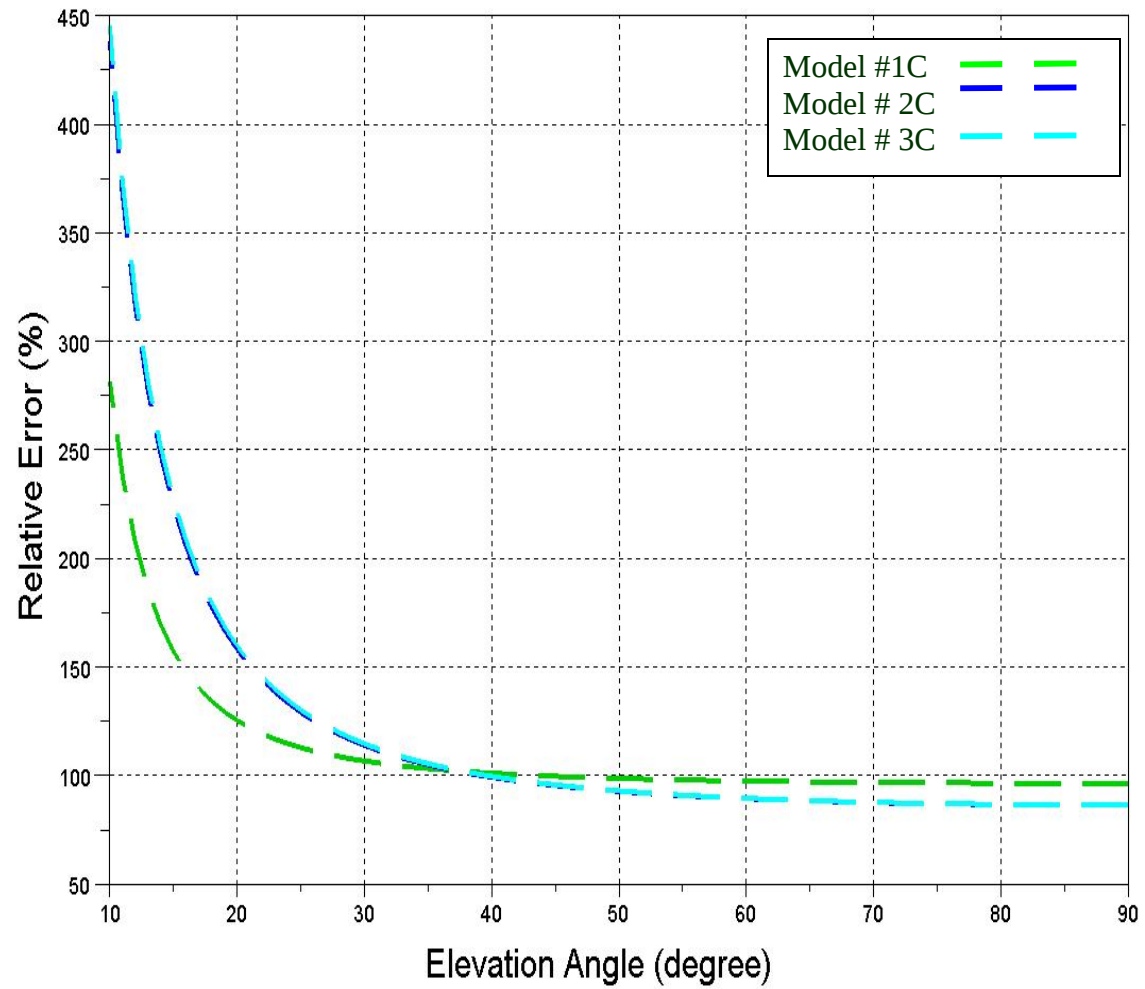Figure B.11– Relative error of the total water vapour content

Figure B.12– Relative error of the total water vapour content

References

1. Tverskoy P.N. Meteorology curse. – L.: Hydrometizdat, 1962. – 692p.

2. Site of NOAA Earth system research library [Electronic resourse]. – http://www.cdc.noaa.gov.

3. Grains Research&Development corporation, Global Navigation Satellite System Australian center for precision agriculture [Electronic resource]. – www.usyd.edu.au/su/agric/acpa.

4. Global Positioning System, Standard Positioning System Service, Signal Specification, 2nd Edition, 1995, page 18, http://www.navcen.uscg.gov

5. http://bolstad.gis.umn.edu/chapt5figs (figures are adapted from «GIS Fundamentals», 3rd Edition, by Paul Bolstad).

6. Collins J. P., (1999). Assessment and development of a tropospheric delay model for air craft users of the global positioning system. Technical report № 203 (188), pp. 13-17.

7. Brunner, F. K.; S. McCluskey, «Tropospheric zenith delay parameters: How many should be estimated in GPS processing.» Australian Journal of Geodesy, Photogrametry and Surveying, vol. 55, pp. 67-75, (1991).

8. Saastamoinen, J. (1972), Atmospheric Correction for the Troposphere and Stratosphere in Radio Ranging of Satellites, In: The Use of Artificial Satellites for Geodesy, Geophysical Monograph Series, AGU, Washington D.C., Vol. 15, 247 -251.

9. Goad, C. C., L. Goodman, «A modified Hopfield tropospheric refraction correction model». Paper presented at the Fall Annual Meeting of the American Geophysical Union, San Francisco, California, December 12-17, (1974).

10. Rocken, C., S. Sokolovskiy, J.M. Johnson and D. Hunt, Improved Mapping of Tropospheric Delays, AMS, Vol 18, 1205-1213, 2001.

11. Tomasz J. Glowacki1, Nigel T. Penna and William P. Bourke, «Validation of GPS-based estimates of integrated water vapour for the Australian region and identification of diurnal variability». Aust. Met. Mag. 55 (2006), P.131-148.